Spectroscopic study of surfactant enhanced organometallic vapor phase epitaxy growth of GaInP

C. M. Fetzer,[a] R. T. Lee, D. C. Chapman, and G. B. Stringfellow
College of Engineering, University of Utah, Salt Lake City, Utah 84112

(Received 10 November 2000; accepted for publication 11 April 2001)

Samples of $Ga_xIn_{1-x}P$ grown by organometallic vapor phase epitaxy on (001) GaAs substrates by addition of TESb demonstrating a lateral superlattice compositional modulation (CM) have been studied by low temperature polarized photoluminescence (PL), power dependent PL, and photoluminescence excitation (PLE) spectroscopy. Strong polarization is observed in the low temperature PL and PLE spectra at Sb concentrations below that where $CuPt_B$ ordering is removed and triple period ordering is produced. Low temperature polarized PL is shown to be the most sensitive optical technique for detecting the presence of CM. The radiative recombination mechanism at low temperature is excitonic, originating from the exponential tail of band gap states observed in the PLE spectra. From the measured band gaps, a continuum model of the band structure allows an estimate of an upper limit of the percent modulation present in the samples. Above Sb/III(v) = 0.01, compositional modulation is the dominant factor determining the low temperature optical properties. The percent fluctuation of composition increases monotonically with increasing Sb during growth. © *2001 American Institute of Physics.* [DOI: 10.1063/1.1378060]

I. INTRODUCTION

Phase separation has long been studied in compound semiconductors. A large positive enthaply of mixing is known to produce regions of immiscibility from bulk thermodynamic considerations.[1] In epitaxial layers, coherence strain may stabilize the single phase alloy in this miscibility gap.[2] However, the proximity of a free surface reduces the coherency stabilization.[3] In an unstable system, two competing types of self-assembled behavior exist, each leading to a reduction of the configurational free energy of a random alloy with a large enthalpy of mixing.[1–4] At the atomic scale, surface reconstruction leads to CuPt ordering, with atomic planes of alternating composition along the {111} directions.[4] On a larger scale, spinodal decomposition leads to compositional modulation (CM) in which a regular superlattice is spontaneously formed.[4] Compositional modulation is observed to be a natural superlattice either: (i) along the growth direction (vertical superlattice) or (ii) perpendicular to the growth direction (lateral superlattice). Both types of CM are frequently observed in III–V semiconductor alloys.[4,5] A schematic diagram of lateral superlattice CM is shown in Fig. 1. When grown on (001) oriented substrates, the superlattice forms along the [110] direction with alternating regions of high and low band gap material extending in vertical wells and barriers along the $[\bar{1}10]$ direction.[5]

Control of the lateral superlattice CM has been demonstrated by many epitaxial methods. Growth of short-period superlattices by molecular beam epitaxy (MBE) has been successfully used to produce self-assembled quantum wires in the $Ga_xIn_{1-x}As$,[6,7] $Al_xIn_{1-x}As$,[8] and $Ga_xIn_{1-x}P$[9] material systems by the so-called strain-induced lateral ordering (SILO) process.[10] Using organometallic vapor-phase epitaxy (OMVPE), a naturally formed lateral superlattice CM has been produced in $Al_xIn_{1-x}As$[11] and $Ga_xIn_{1-x}As$[12] single layers. The period of both natural and SILO formed superlattices was observed to range from 100 to 400 Å.[5] Recently, the use of surfactants has been demonstrated to control phase separation and has led to a lateral superlattice CM in the OMVPE growth of $Ga_xIn_{1-x}P$.[13] The surfactant enhanced superlattices have a much larger period, of about 120 nm, but maintain the same orientation as those formed by other methods. Surfactant mediated growth may be used to control the CM amplitude by controlling the growth rate and the amount and type of surfactant.[14] Simultaneously, an ordered phase, with triple the period of the lattice along the {111} A directions, was observed in the Sb modified samples.[13,15,16] Recent results suggest that the triple period ordering (TPO) has little impact on the low temperature optical properties.[13] A hypothesis which is in direct contrast to previous studies, where TPO had been hypothesized to be responsible for an observed band gap reduction,[15–18] much like that known to occur for CuPt ordering.[4,19] The question of which microstructure is responsible for the optical properties is nontrivial since both microstructures, ordering and CM, may be used to engineer the properties of structures for advanced optoelectronic devices.[4,5,10,20] The resolution of this issue facilitates the use of isoelectronic surfactants as a means of engineering the properties of III–V epitaxial layers during their growth.

All of the observed microstructures impact optical properties. It follows then that an optical means may be used to distinguish the presence of a given structure. The confirmation of the presence of a given structure must be made with an alternate and established technique such as transmission electron microscopy (TEM)[4,5] or x-ray diffraction.[12] These techniques for microstructure characterization are either destructive, consuming the sample, in the case of TEM, or may not be readily available. Understanding the relation of key

[a]Electronic mail: cfetzer@spectrolab.com

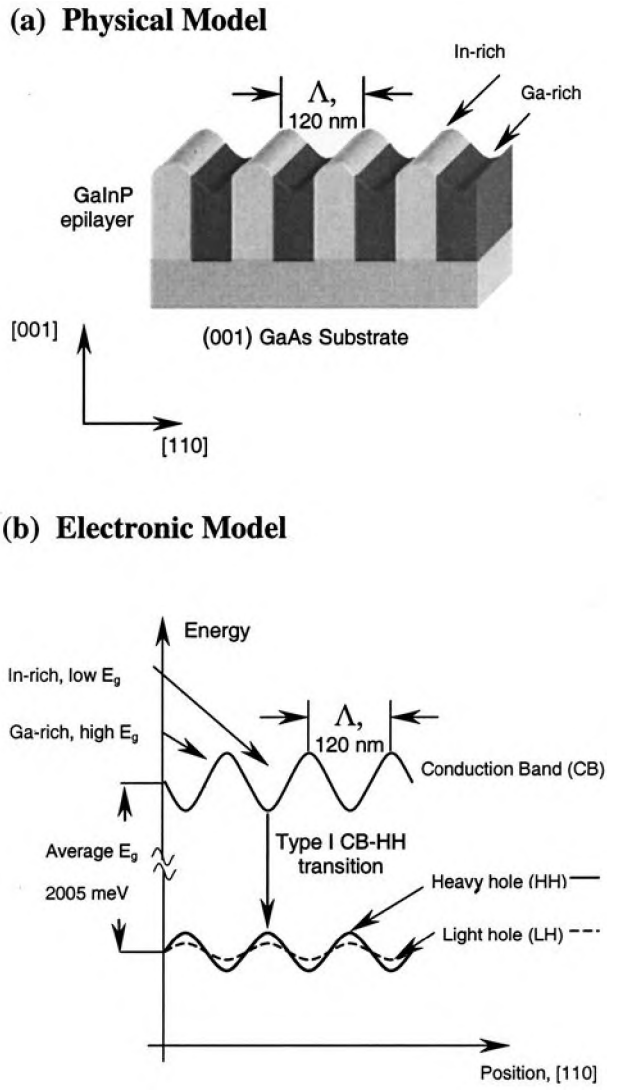

FIG. 1. Schematic diagram of lateral superlattice CM in GaInP epilayers. (a) The alloy epilayer is divided into a superlattice along the [110] direction of alternating $Ga_{x+\delta}In_{1-x-\delta}P$, Ga-rich regions, represented by dark areas, and $Ga_{x-\delta}In_{1-x+\delta}P$, In-rich regions, represented by the light areas. The band gap may be represented by alternating high and low band regions in a sine wave along the [110] direction shown in (b). The valence band shows a split between the heavy hole (HH) and light hole bands, with the HH band higher in energy in the In-rich (low band gap) regions.

optical properties to the microstructure of these layers gives a researcher a nondestructive method to characterize the layer.

In all the microstructures, the band gap, as measured by photoluminescence (PL), is observed to decrease in samples with either microstructure.[4,5] In samples exhibiting CM, strong polarized PL perpendicular to the superlattice (the $[\bar{1}10]$ is the stronger orientation) is also reported.[5] The strength of the PL polarization (reported as the ratio of the two orientations) has been observed to reach values as high as 40 and is strong even for small amplitudes of CM.[5,13,21] Samples exhibiting strong CuPt ordering also show polarized PL; however, the intensity is stronger for the [110] orientation, oriented opposite that of CM.[19] Additionally, the strength of the polarization for CuPt ordering may reach a maximum value of only 3 for fully ordered material.[22] One would assume then that triple period ordering would be limited to a similar value. This difference in polarized PL in strength and orientation for the observed microstructures in Sb modified GaInP may be used to resolve the issue as to which microstructure dominates the low temperature optical properties, CuPt ordering, triple period ordering, or CM.

This article describes the optical properties of surfactant induced CM in epitaxial $Ga_xIn_{1-x}P$ (hereafter GaInP). The experimental relationship between the amount of surfactant and the magnitude of the compositional fluctuation of the CM will be explored. Using low temperature PL and photoluminescence excitation (PLE) spectroscopies both the low and high band gap regions of CM may be probed. Comparison of the results of the samples grown without Sb, known to be $CuPt_B$ ordered, with those grown with Sb may be used to distinguish the onset of CM. The results are correlated to a theoretical model covering both high and low band gap regions and provide an upper estimate of the percent fluctuation of the CM present in the samples.

II. EXPERIMENT

All samples were grown in a horizontal flow atmospheric pressure OMVPE reactor. The details of the growth method have been given previously.[23] The 0.4-μm-thick epitaxial layers of GaInP were grown under conditions giving nominal lattice match to semi-insulating (001) GaAs substrates having misorientation of either 0° (singular) or 3° to the [111]B (3°_{B} vicinal). The lattice mismatch determined from x-ray diffraction was $\Delta a/a < 10^{-3}$ for the samples used in this study. A control sample was grown on (511)A oriented semi-insulating GaAs to produce nearly disordered and uniform (i.e., no CM) GaInP without the introduction of a surfactant.[24,25] Trimethylgallium, ethyldimethylindium, and tertiarybutylphosphine were used as precursors. The growth rate was constant at 1 μm/h. The V/III ratio was held at 40. Triethylantimony, TESb, was used in low concentrations as a surfactant. The concentration is specified as the ratio of TESb to total group III partial pressure in the vapor [Sb/III(v)]. Because Sb is nonvolatile, this ratio reflects the amount of Sb on the surface of the epilayer for a given growth time. To compare results reported using this ratio with those of previously published studies using Sb/P(v),[15,16,24] one simply multiplies the value by the V/III ratio. The use of surfactant Sb has been previously observed to induce disordering, TPO, and CM in GaInP, depending on Sb/III(v).[13–16]

Polarized PL was studied by focusing light from an argon ion laser (488 nm) to a spot size 0.2 mm in diameter for a total excitation intensity of 30 W/cm^2. For some experiments, the excitation intensity was reduced by using neutral density filters. The sample temperature was controlled using a closed-cycle He refrigerator and cold finger combination. The sample temperature was nominally 12 K for most measurements. Higher temperatures were obtained by heating the cold finger using a resistive element and a programable temperature controller. The luminescence was collected by lenses and passed through a rotating polarizer film to select the PL orientation, along either the [110] or the $[\bar{1}10]$ direc-

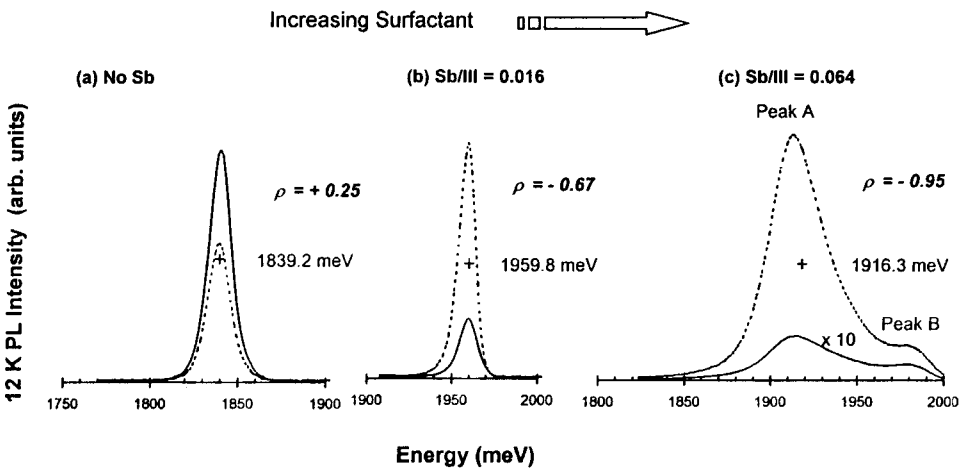

FIG. 2. Polarized PL spectra taken at 12 K for increasing amounts of Sb, denoted Sb/III(v). The dashed line is the spectrum polarized along [$\bar{1}$10] and the solid line is for the perpendicular, [110], polarization. The peak energy and polarization are indicated for each spectrum. For the highest value of Sb/III(v) shown, Sb/III(v)=0.064, (c), the [110] orientation has been multiplied by a factor of 10 for clarity. In that spectrum, a low-energy peak and high-energy shoulder are labeled as peaks A and B, respectively.

tion. The resulting PL was dispersed through a 0.5 m monochromator (SPEX 500M) and collected onto an uncooled bialkali photomultiplier tube. Standard lock-in amplification techniques were used to reduce the noise and amplify the signal. All spectra were corrected for system response. PLE was collected using the same system with the sample at 12 K. A single wavelength of light from a 300 W filament lamp was selected by a 0.5 m monochromator, polarized, and focused onto the sample with an incident intensity of approximately 1 W/cm^2. The luminescence from the PLE experiment was collected unpolarized with the same system used for regular PL.

III. EXPERIMENTAL RESULTS AND DISCUSSION

A. Photoluminescence

Figure 2 shows the basic, low temperature polarized PL for selected samples with increasing Sb concentration. In each spectrum, the polarization, ρ, is reported as

$$\rho = \frac{I_{[110]} - I_{[\bar{1}10]}}{I_{[110]} + I_{[\bar{1}10]}}. \tag{1}$$

$I_{[\bar{1}10]}$ and $I_{[110]}$ are the integrated PL intensities with the polarizer oriented along the [$\bar{1}$10] and [110] directions. The spectrum for the sample with no Sb [Fig. 2(a)] has a peak energy of 1839.2 meV and a polarization, ρ, of +0.25. Both values are typical of $CuPt_B$ ordered material with order parameter of 0.6, as reported previously.[24] The addition of small amounts of Sb has a dramatic effect on the polarized PL spectrum. For Sb/III(v)=0.016 [Fig. 2(b)], the peak energy corresponds to nearly disordered GaInP at 1959.8 meV, comparable to that of the (511)A control sample at 1968 meV. The full widths at half maximum (FWHM) are also comparable at 12 meV for Fig. 2(b) and 14 meV for the control sample. The polarization of the sample with Sb/III(v)=0.016 becomes −0.672, indicating a stronger polarization along [$\bar{1}$10]. The polarization of the control sample is +0.15, typical of weak $CuPt_B$ ordering. The strong polarized PL shows that the sample grown with Sb/III(v) =0.016 is not just weakly $CuPt_B$ ordered as represented in earlier reports.[15,16,24] Both the polarization strength and direction indicate the possible presence of lateral superlattice CM.[5,15] In TEM studies, which included this sample, only the weak $CuPt_B$ ordering was observed, comparable to that observed in the control sample.[15,16,24] The TEM studies may have missed the presence of CM altogether, since at the time, there was no direct examination for its presence in any of the Sb modified layers. The small FWHM of the PL also indicates that the CM amplitude may be very weak. If the CM is regional on the sample, then the small volume probed by TEM may not have contained any CM structure. Only in subsequent TEM examination of other samples at slightly higher concentrations was CM discovered.[13] Atomic force microscopy (AFM) detected the presence of surface undulations on this same sample, extending along the [$\bar{1}$10] direction.[13] Such undulations are also typical of the presence of CM.[5] The sample that exhibited TPO in the earlier reports, for Sb/III(v)=0.064 is shown in Fig. 2(c). The energy of the dominant peak (A) is 1916.3 meV and a high energy shoulder is also present, labeled peak B. The spectrum is very polarized, with ρ=−0.95, a ratio of integrated intensities along the [$\bar{1}$10] and [110] directions of 41–1. Although the sign is correct (ρ<0) for an A variant of {111} ordering,[4,19] the polarization magnitude is too strong to be due to the presence of TPO. This same sample has also been confirmed to contain strong CM microstructure by TEM and AFM.[13] The dramatic polarization and band gap reduction are all consistent properties of the CM microstructure. The strong polarization present in the sample grown at Sb/III(v) =0.016 [Fig. 2(b)] may also indicate the presence of a weaker CM amplitude in that sample.

The observation that a strong PL polarization oriented along the [$\bar{1}$10] correlates to the presence of a CM microstructure may be applied to observe the onset of CM as a function of Sb/III(v). Figure 3 summarizes the dependence of the 12 K PL peak energy and polarization, ρ, on Sb/III(v) during growth for all samples included in this study. The PL spectra show a strong negative polarization above Sb/III(v) =0.01, indicating a strong polarization in the [$\bar{1}$10] direction occurs at this Sb/III(v). This point is below the concentration at which the highest band gap is observed at Sb/III(v) =0.016. TED patterns indicate the presence of $CuPt_B$ ordering in this same sample.[24] The polarization result suggests the simultaneous presence of CM in the samples, but this has

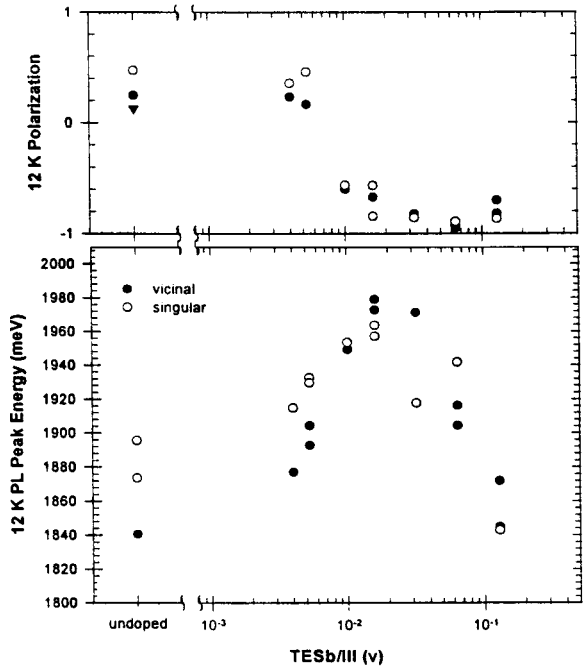

FIG. 3. Summary of 12 K PL peak energy (a) and polarization, ρ, (b) for increasing amounts of surfactant. Filled circles represent vicinal samples and open circles denote singular samples. The polarization of the (511)A control sample is shown, represented by the filled triangle. The polarization has switched sign at Sb/III(v)=0.01 a concentration lower than that giving the highest peak energy at Sb/III(v)=0.016.

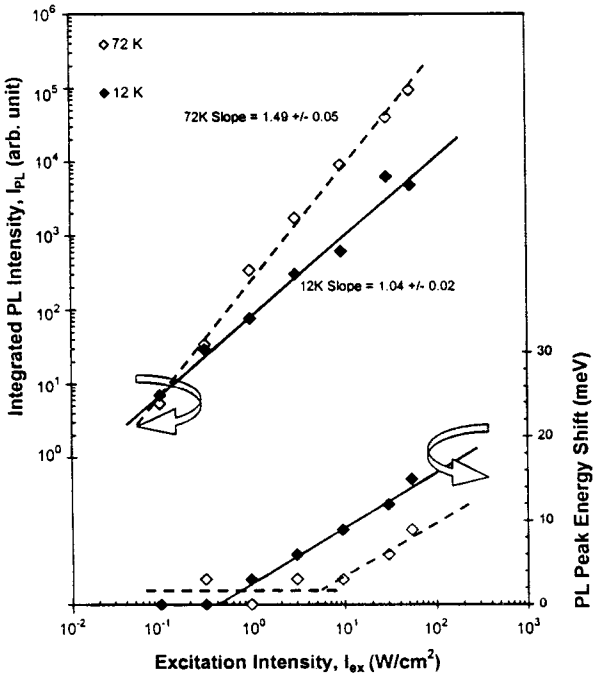

FIG. 4. Results of varying the incident laser intensity on the sample grown with Sb/III(v)=0.064 at measured temperatures of 12 K (filled markers) and 72 K (open markers). The upper figure shows the variation in integrated PL intensity for the [$\bar{1}$10] direction. The slope of the log–log plot at 12 K (solid line) is 1.04, while at 72 K (dashed line) it is 1.49. The lower figure shows the peak energy shift from the lowest measured value vs excitation intensity for both temperatures.

not been confirmed by another means. Above Sb/III(v) =0.016, the polarization becomes more negative as the peak energy decreases. For Sb/III(v)=0.064, the polarization reaches a maximum of $\rho=-0.95$ and the PL peak reaches 1916 meV as seen in Fig. 2(c). At higher Sb concentrations, the peak energy is observed to decrease further to 1807 meV, below that of even the most $CuPt_B$ ordered sample at 1839 meV. TPO is only observed for Sb/III(v)>0.064 and the strength is observed to decrease for Sb/III(v)=0.128. Both observations show that TPO is not responsible for the observed band gap reduction or strong polarization present in the PL spectra. Again, a strong indication that polarization is directly related to the only consistently observed microstructure, CM.

Another factor known to affect the PL peak energy is Sb incorporation. The Sb concentration in the solid may be measured using secondary ion mass spectroscopy and is at most only 0.1% for Sb/III(v)=0.128. The resulting band gap reduction due to alloying is at most 10 meV, if the Sb is assumed to incorporate uniformly.[26] There is the possibility that Sb is not uniform throughout the layers. The absolute positional composition has not been measured and Sb may indeed be nonuniformly distributed in the layer. But, the overall concentration of Sb is small. If Sb preferentially segregated into the regions of lowest band gap, it would serve to enhance the observed properties of a CM microstructure of the underlying alloy, reducing the band gap in the lowest regions and increasing the strain splitting the valence band of those regions thus increasing the observed polarization.

B. Temperature and power dependent PL

Changing the excitation intensity can be used as a tool to clarify the recombination mechanism and the microstructure, CM or TPO, responsible of the PL. By fitting the integrated PL intensity, I_{PL}, to the excitation intensity, I_{EX} using the relation

$$I_{PL}=\eta I_{EX}^{\beta}, \tag{2}$$

one may determine the radiative recombination mechanism.[27,28] Results for the sample grown with Sb/III(v)=0.064, are shown in Fig. 4. PL for both polarizer orientations show a common exponent at both temperatures, 12 and 72 K, so only the [$\bar{1}$10] polarization data are plotted. At 12 K an exponent of 1.04±0.02 indicates that free carriers recombine as excitons.[28] At 72 K, the exponent increases to 1.49±0.05, indicating a combination of excitonic and free carrier band-to-band recombination.[27–29] The increase in exponent at 72 K may be explained by thermalization of a portion of the exciton population to produce free electrons and holes. The lower portion of Fig. 4 shows the PL peak energy shift as a function of excitation intensity. The 12 K PL peak energy begins to shift almost immediately with increasing excitation intensity. This effect is attributable to state filling of the exponential tail of the exciton band caused by strong localization.[30,31] State filling of a localized exciton band tail has also been observed in other samples showing CM.[31] Figure 1(b) gives a schematic model of the conduction and valence bands for a lateral superlattice CM. At low temperatures, photogenerated carriers relax into the lowest band

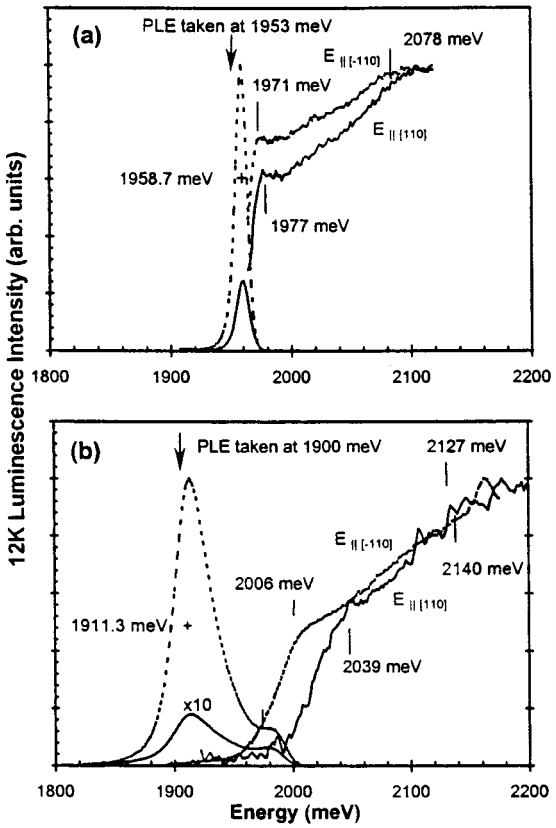

FIG. 5. Polarized PL and PLE spectra for samples at Sb/III(v)=0.016, (a) and Sb/III(v)=0.064, (b). The [$\bar{1}$10] oriented PLE spectra and polarized PL spectra are indicated by the dashed lines. The arrows indicate the energy at which the PLE spectra were taken.

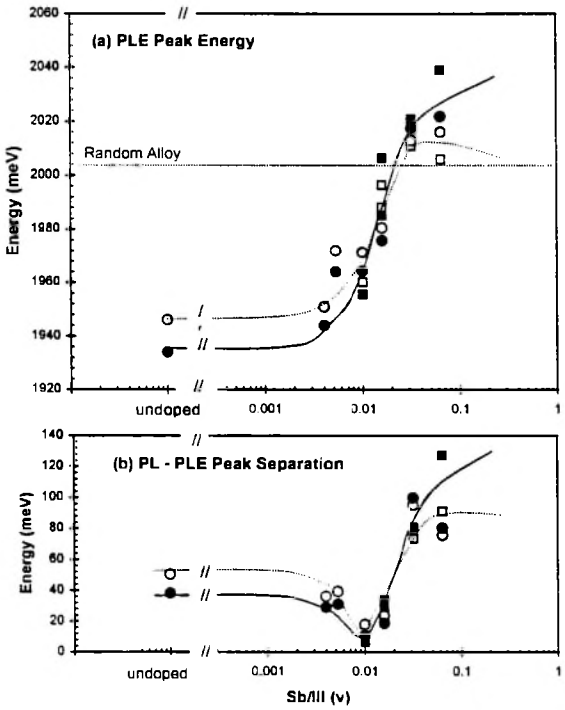

FIG. 6. Summary of PL and PLE peak energies vs Sb/III(v). The filled points are for singular samples and the open points are for vicinal samples. The lines drawn through the data points are meant to guide the eye. The dashed lines represent data for the polarizer along the [$\bar{1}$10] orientation and solid lines are for the polarizer along the [110]. Squares represent data from vicinal samples while circles represent data from singular samples. The energy of the random alloy is denoted by the horizontal dotted line at 2.005 eV.

gap regions, where they become trapped and recombine as excitons. The band tailing occurs because of the nonuniformity of the CM. The PL arises from the deepest lying states. At 72 K only a portion of the carriers recombine as excitons, requiring a higher excitation intensity to fill the states and shift the peak energy. As seen in the figure, at 72 K the PL peak begins to shift at an order of magnitude higher excitation than at 12 K.

C. Photoluminescence excitation

PL probes only the lowest band gap tails of the CM structure. An additional feature of CM is the existence of higher band gap regions as seen schematically in Fig. 1(b). To study these high band gap regions, an absorption type spectroscopy must be employed. Here, PLE was used to probe the higher band gap regions. PLE spectra for both samples with Sb/III(v)=0.016 and Sb/III(v)=0.064 are shown in Figs. 5(a) and 5(b), respectively. In both samples, the PLE was detected at slightly below the peak energy to allow the detection of the lowest absorption edge. The PLE spectra for the sample with Sb/III(v)=0.016 [Fig. 5(a)], are nearly identical for both polarizations. Each spectrum shows an exciton resonance near the band edge, located at a slightly higher energy for the [110] polarization (1977 meV) as compared to that for the [$\bar{1}$10] polarization (1971 meV). This difference is significant, since it shows the valence band splitting predicted for CM in the schematic of Fig. 1(b) in the high band gap regions. The observed valence band splitting is reversed from that typical of CuPt ordering, where the [110] edge is at a lower energy than for the [$\bar{1}$10].[32] The PLE spectrum of the sample with Sb/III(v)=0.064 is shown in Fig. 5(b). The entire [110] spectrum has now shifted relative to the [$\bar{1}$10] spectrum. The shoulder is at 2039 meV for the [110] polarized spectrum and is at a lower energy of 2006 meV for the [$\bar{1}$10] polarization. Both values are higher than for completely random GaInP lattice matched to GaAs.[4,19,32] The PLE edge arises from the Ga-rich, higher band gap, regions of the CM. The shape of the PLE spectra below the edge clearly demonstrates the same exponential tail described earlier and shows that the PL spectra originate deep within this tail as deduced earlier. Taking the shoulder as the fundamental absorption edge, Stoke's shifts between the PL and PLE of 94.7 meV and 127.7 meV are measured for the [110] and [$\bar{1}$10] orientations, respectively. The shape of the PLE edge is different from that observed in $CuPt_B$ ordered samples, where two peaks or inflections are observed for each polarizer orientation,[32] directly indicating that the PLE spectra do not originate from a form of ordering. The [$\bar{1}$10] edge is lower in energy since the topmost valence band in the Ga-rich regions allows only transitions with the polarization oriented along the wells.[34]

The PLE peak energies and PL–PLE peak separations (Stoke's shifts) for the entire series of samples are plotted vs Sb/III(v) in Figs. 6(a) and 6(b), respectively. In the

undoped samples, the Stoke's shift is seen to be 25 ± 5 meV, with a splitting between the [110] and [$\bar{1}$10] polarizations that is typical of that produced by CuPt ordering in GaInP, as reported earlier.[32] The [110] polarization edge is observed to be lower in energy than the [$\bar{1}$10] edge, consistent with strong $CuPt_B$ ordering.[32] As the Sb concentration increases the separation between the edges for the two polarizations decreases monotonically, as does the Stoke's shift, all in agreement with the disordering proposed in earlier work on Sb modified GaInP.[15,16,24] At the same concentration of Sb where the PL polarization is observed to reverse, Sb/III(v) $=0.010$ (Fig. 3), the Stoke's shift becomes nearly zero. Above this concentration, the [$\bar{1}$10] orientation becomes the lower energy edge. The reversal in PLE edges observed here explains the observed polarization reversal in Fig. 3. If the lowest energy transition is strongly [$\bar{1}$10] oriented, the radiative recombination of the low temperature PL would also become oriented the same direction. The PLE results show that as $CuPt_B$ ordering is being removed by the addition of Sb, the CM is simultaneously increasing in strength. With the onset of strong CM above Sb/III(v)>0.03, a large separation between the [110] and [$\bar{1}$10] edges is observed, with the energies clearly exceeding the band gap of the random alloy (2.005 eV). Both singular and vicinal samples follow the same trend in Fig. 6, indicating that a slight substrate misorientation has little effect on the surfactant induced CM, as was observed previously in epilayers showing lateral superlattice CM grown by MBE and the SILO method.[33]

IV. DISCUSSION

The experimental data presented earlier demonstrate that a lateral superlattice CM is present in GaInP epilayers when grown with Sb/III(v)>0.01. The increase in polarization of the PL and the decrease in PL peak energy with increasing Sb/III(v) qualitatively indicate that the low band gap regions become more In rich as the amount of Sb is increased during growth. Simultaneously from the PLE results, the valence band splitting and peak energy of the Ga-rich regions increase, indicating that the high band gap regions become more Ga rich. The effects in both low and high band gap regions are linked by defining the compositional deviation from lattice match as the CM amplitude, δ. As observed by TEM and shown in Fig. 1, the composition at any point may be modeled as a wave along the [110] direction with a periodicity of 120 nm.[13,14]

Knowing the initial composition profile, the effects on the band gap may be calculated and the results compared with the PL and PLE results. Many models have been posed in the literature for lateral superlattice CM.[5,34–36] The model best suited to the comparison here is a continuum model based on the **k·p** description of the semiconductor band structure.[34] Material parameters for the alloy regions may be linearly interpolated from values of the end-point binaries, GaP and InP, and are tabulated elsewhere.[34] The wave profile may be modeled as either a square wave or a sine wave. A more accurate composition profile would be a modified square wave with graded interfaces between the regions.[34–36] The actual profile is unknown, so a sine wave is assumed since it is the simplest approximation of the graded interfaces between regions. Using that profile, the amplitude, δ, denotes the largest deviation of the composition at the center of each Ga-rich ($Ga_{0.515+\delta}In_{0.485-\delta}P$) and In-rich ($Ga_{0.515-\delta}In_{0.485+\delta}P$) region.

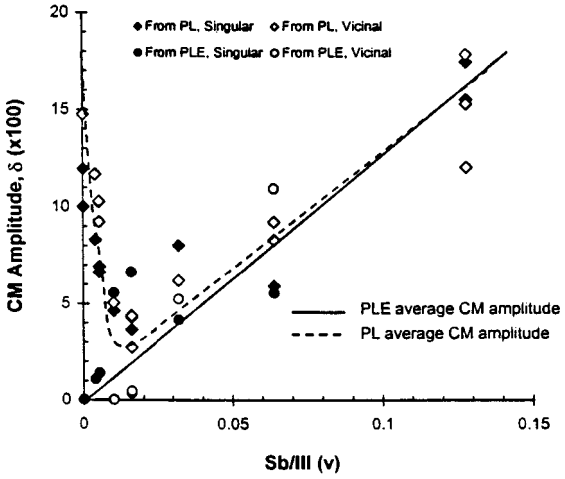

FIG. 7. CM amplitude, δ, vs Sb/III(v) calculated from energies of the PLE [110] edge (diamonds) and PL peak energy (circles). Filled and open data points represent singular and vicinal samples, respectively. Average values of the CM amplitude are indicated by lines as calculated from PL peak energies (dashed line) and PLE [110] edge energies (solid line).

With these assumptions, the initial compositional profile is input into the model and the resulting band gaps are calculated for a given CM amplitude, δ. Here, the inverse problem is required. Starting with the band gaps of both In-rich and Ga-rich regions, the PL peak energy and the PLE [110] edge energy, respectively, are used to calculate, δ, in the sample. The effects of $CuPt_B$ ordering may be assumed to be linearly superimposed on those of the CM. The amount of band gap reduction in the PLE due to the ordering may be removed empirically by using the valence band splitting between the [110] and [$\bar{1}$10] edges, in samples where the [110] orientation is lower in energy.[33] Prior to calculating the CM amplitude, the band gap reduction due to ordering is added to the PLE edge energy. For comparison, the values calculated from the PL peak energy were not corrected. It is assumed that TPO has little effect on the relevant band structure.

Using such a complex calculation presents many inaccuracies into the calculated values. There many sources of error in the model. For these reasons, this calculation presents at best only an estimate of the compositions of the CM regions.

The results of the calculation are plotted as the CM amplitude, δ, vs Sb/III(v) in Fig. 7. The dashed and solid lines show the average value of the calculation for each data set, PL peak energy and PLE [110] edge energy, respectively. Below the critical concentration of Sb/III(v)$=0.01$, the values for the uncorrected PL data deviate significantly from the corrected PLE data. In this case, the $CuPt_B$ ordering is the dominant microstructure and the CM model is not valid in this region. Above Sb/III(v)$=0.01$, the average deviation calculated for both PL peak energy and PLE shoulder energy converge. Both averages increase monotonically with increasing Sb/III(v). At Sb/III(v)$=0.128$ the CM amplitude,

δ, reaches a maximum with an average value of 0.17. At this Sb concentration, the GaInP epilayer has segregated into regions of $Ga_{0.68}In_{0.32}P$ (Ga rich) and $Ga_{0.34}In_{0.66}P$ (In rich). At those compositions, the strain energy (due to the lattice mismatch with the substrate and between regions of different compositions) of the individual regions is significant and leads to the formation of many strain-related defects. As was observed at Sb/III(v) = 0.128, the resulting high defect density reduces the overall PL intensity. Many stacking faults and apparent strain regions at the epilayer-substrate interface are also observable in bright-field TEM images for samples above Sb/III(v) = 0.064.[13,14,16] The overall optical quality of the samples drops above that concentration due to the increased CM amplitude.

V. CONCLUSIONS

In summary, the optical properties due to surfactant enhanced lateral superlattice CM formation in GaInP have been explored. Results of 12 K polarized PL show that above Sb/III(v) = 0.01, a polarization reversal occurs as the CM becomes the dominant microstructure producing the optical properties. The use of the polarization reversal in the 12 K PL is the most sensitive optical technique for identifying the onset of the CM in the samples. The PL in the CM samples originates from localized excitons in an exponential density of states tail. PLE results show that above Sb/III(v) = 0.01, the CM is also detected from the high band gap regions. The peak energies from the PL and PLE results have been used to demonstrate that above Sb/III(v) = 0.01, the deviation from lattice match increases monotonically with increasing Sb/III(v), reaching a maximum of 0.17. Above Sb/III(v) = 0.064, the optical quality of the samples drops, due to the strain at the epilayer-substrate interface and between composition regions forming defects which act as nonradiative recombination centers.

ACKNOWLEDGMENTS

The authors would like to thank the Department of Energy for their financial support of this work. Also, the authors wish to thank Professor P. Craig Taylor and Dr. J. Kevin Shurtleff for their contribution by careful reading of the manuscript and helpful suggestions.

[1] G. B. Stringfellow, J. Cryst. Growth **52**, 194 (1982).
[2] G. B. Stringfellow, J. Electron. Mater. **11**, 903 (1982).
[3] F. Glas, J. Appl. Phys. **62**, 3201 (1987).
[4] A. Zunger and S. Mahajan, in *Handbook of Semiconductors*, edited by T. S. Moss (Elsevier Science, Amsterdam, 1994), Vol. 3, p. 1399.
[5] J. Mirecki Millunchick *et al.*, MRS Bull. **22**, 38 (1997).
[6] S. T. Chou, K. C. Hsieh, K. Y. Cheng, and L. J. Chou, J. Vac. Sci. Technol. B **13**, 650 (1995).
[7] K. Y. Cheng, K. C. Hsieh, and J. N. Baillargeon, Appl. Phys. Lett. **60**, 2892 (1993).
[8] J. Milrecki Millunchick *et al.*, Appl. Phys. Lett. **70**, 1402 (1997).
[9] K. C. Hsieh, J. N. Baillergeon, and K. Y. Cheng, Appl. Phys. Lett. **57**, 2244 (1990).
[10] P. J. Pearah, A. C. Chen, A. M. Moy, K. C. Hsieh, and K. Y. Cheng, IEEE J. Quantum Electron. **30**, 608 (1994).
[11] S. W. Jun, T. Y. Seong, J. H. Lee, and B. Lee, Appl. Phys. Lett. **62**, 3443 (1996).
[12] R. D. Twesten *et al.*, Bull. Am. Phys. Soc. **41**, 693 (1996).
[13] C. M. Fetzer, R. T. Lee, S. W. Jun, G. B. Stringfellow, S. M. Lee, and T. Y. Seong, Appl. Phys. Lett. **78**, 1376 (2001).
[14] R. T. Lee, C. M. Fetzer, S. W. Jun, D. C. Chapman, G. B. Stringfellow, S. M. Lee, and T. Y. Seong, J. Cryst. Growth (submitted).
[15] C. M. Fetzer, R. T. Lee, J. K. Shurtleff, G. B. Stringfellow, S. M. Lee, and T. Y. Seong, Appl. Phys. Lett. **76**, 1440 (2000).
[16] T. Y. Seong, S. M. Lee, R. T. Lee, and G. B. Stringfellow, Surf. Sci. **457**, L381 (2000).
[17] A. Gomyo, K. Makita, I. Hino, and T. Suzuki, Phys. Rev. Lett. **72**, 673 (1994).
[18] A. Gomyo, K. Makita, I. Hino, and T. Susuki, J. Cryst. Growth **150**, 533 (1995).
[19] A. Mascarenhas, S. Kurtz, A. Kibbler, and J. M. Olsen, Phys. Rev. Lett. **63**, 2108 (1989).
[20] D. E. Wohlert, A. M. Moy, L. J. Chou, K. Y. Cheng, and K. C. Hsieh, J. Vac. Sci. Technol. B **16**, 1352 (1998).
[21] D. E. Wohlert and K. Y. Cheng (private communication).
[22] S. H. Wei and A. Zunger, Appl. Phys. Lett. **64**, 1676 (1994).
[23] H. Murata, I. H. Ho, L. C. Su, Y. Hosokawa, and G. B. Stringfellow, J. Appl. Phys. **79**, 6895 (1996).
[24] J. K. Shurtleff, R. T. Lee, C. M. Fetzer, and G. B. Stringfellow, Appl. Phys. Lett. **75**, 1914 (1999).
[25] G. B. Stringfellow, MRS Bull. **22**, 27 (1997).
[26] D. H. Jaw, M. J. Zou, Z. M. Fang, and G. B. Stringfellow, J. Appl. Phys. **68**, 3538 (1990).
[27] S. Jin, Y. Zheng, and A. Li, J. Appl. Phys. **82**, 3870 (1997).
[28] J. E. Fouquet and A. E. Siegman, Appl. Phys. Lett. **46**, 280 (1985).
[29] E. D. Jones, D. M. Follstaedt, S. K. Lyo, and R. P. Schnieder, Jr., Mater. Res. Soc. Symp. Proc. **281**, 61 (1993).
[30] E. Cohen and M. D. Sturge, Phys. Rev. B **25**, 3828 (1982).
[31] M. Sugisaki, H.-W. Ren, K. Nishi, S. Sugou, and Y. Masumoto, Phys. Rev. B **61**, 16040 (2000).
[32] P. Ernst, C. Geng, F. Scholz, and H. Schweizer, Phys. Status Solidi B **193**, 213 (1996).
[33] A. C. Chen, A. M. Moy, L. J. Chou, K. C. Hsieh, and K. Y. Cheng, Appl. Phys. Lett. **66**, 2694 (1995).
[34] Y. Zhang and A. Mascarenhas, Phys. Rev. B **57**, 12 245 (1998).
[35] A. Mascarenhas, R. G. Alonso, G. S. Horner, S. Froyen, K. C. Hsieh, and K. Y. Cheng, Superlattices Microstruct. **12**, 57 (1992).
[36] T. Mattila, L. W. Wang, and A. Zunger, Phys. Rev. B **59**, 15 270 (1999).